Robotica: (2021) volume 39, pp. 1791–1805. © The Author(s), 2021. Published by Cambridge University Press.
doi:10.1017/S0263574720001502

Intelligent Target Visual Tracking and Control Strategy for Open Frame Underwater Vehicles

Chaoyu Sun†, Zhaoliang Wan‡, Hai Huang‡*, Guocheng Zhang‡, Xuan Bao‡, Jiyong Li‡, Mingwei Sheng‡ and Xu Yang¶

†*Hospital of Harbin Medical University, Harbin 150026, China. E-mail: sary_1023@126.com*
‡ *National Key Laboratory of Science and Technology on Underwater Vehicle, Harbin Engineering University, Harbin 150001, China. E-mails: wanzhaoliang@hrbeu.edu.cn, zhangguocheng168@sina.com, 928755274@qq.com, lijiyong@hrbeu.edu.cn, smwsky@hrbeu.edu.cn*
¶ *State Key Laboratory of Management and Control for Complex System, Institute of Automation, Chinese Academy of Science, Beijing 100190, China. E-mail: xu.yang@ia.ac.cn*

(Accepted December 17, 2020. First published online: February 23, 2021)

SUMMARY
Visual tracking is an essential building block for target tracking and capture of the underwater vehicles. On the basis of remotely autonomous control architecture, this paper has proposed an improved kernelized correlation filter (KCF) tracker and a novel fuzzy controller. The model is trained to learn an online correlation filter from a plenty of positive and negative training samples. In order to overcome the influence from occlusion, the improved KCF tracker has been designed with an added self-discrimination mechanism based on system confidence uncertainty. The novel fuzzy logic tracking controller can automatically generate and optimize fuzzy rules. Through Q-learning algorithm, the fuzzy rules are acquired through the estimating value of each state action pairs. An S surface based fitness function has been designed for the improvement of learning based particle swarm optimization. Tank and channel experiments have been carried out to verify the proposed tracker and controller through pipe tracking and target grasp on the basis of designed open frame underwater vehicle.

KEYWORDS: Remotely autonomous underwater vehicle; Kernelized correlation filter tracking; Learning based fuzzy controller.

1. Introduction

For the exploration and operation in the unstructured oceanic environment, underwater vehicles[1] can play great roles in helping human beings with oceanic engineering, environmental perception and marine science research.[2] Although underwater vehicles can be classified into Autonomous Underwater Vehicle (AUV)[3] and Remotely Underwater Vehicle (ROV),[4] many researchers are currently making research on remotely autonomous control to improve ROV's working efficiency. Target tracking represents one of the most important capabilities for underwater vehicles to carry out underwater autonomous tasks. It not only requires the vehicle continuously classifying and locking the target,[5] but also requires accurately following control.[6]

* Corresponding author. E-mail: haihus@163.com

https://doi.org/10.1017/S0263574720001502 Published online by Cambridge University Press

Visual tracking is an essential building block for target following and capture of the underwater vehicles.[7] The tasks usually initialize a bounding box surrounding the target in the first frame and then estimate its states in the next frames. Significant efforts have been made over the past decades in the field of tracking research, including motion model, the model updater, and the observation model. Some representative trackers include Gaussian process,[8] structured output of Support Vector Machine (SVM),[9] multi-instance learning[10] and deep learning.[11–13]

However, most visual tracking algorithms are onshore oriented, the underwater visual tracking algorithms progress slowly with few literatures reports, due to the complexity of the underwater environment and the limits of underwater robotic hardware. Mean-shift based methods are the most commonly used underwater tracking algorithms because of their simplicity and small amount of calculation. Camshift tracker was applied in a biomimetic robotic fish with a stable head control.[14] However, they are not robust enough and prone to drift for the tracking of underwater marine organism especially when the objects are close and similar. Recently, the Correlation Filter (CF) trackers,[15,16] which can be solved in the discrete Fourier transform efficiently, have demonstrated very promising performance. Deep convolutional network tracking is also an option.[17] But it is more complex for embedded systems. Occlusion is still a problem that could result in tracking failure or drift. When occlusion occurs, the observation model of the tracking target is updated due to the target change. Therefore, the occlusion problem can often result in tracking and operation failure. In order to solve these problems, this article is going to design an improved Kernelized Correlation Filters (KCF) based tracker with feedback mechanism to take the advantage of the robustness and the accuracy of CF trackers and prevent the tracking drift from occlusion.

In order to realize precise target tracking control, numerical controllers have been designed to drive the underwater vehicles to the desired path. Bidyadhar Subudhi et al.[18] presented an output feedback controller for AUV on the basis of its dynamics. Xue Qi et al.[19] proposed a novel target tracking control algorithm on the basis of Lyapunov and back stepping technique with the application of hyperbolic tangent functions. The generated amplitude limit control signals can prevent actuators from saturation and reduce tracking errors. Chao Shen et al.[20] proposed a non-linear model predictive control method to realize AUV trajectory, and incorporate the log barrier functions into cost function to handle the realistic constraints from the thruster.

To further improve the controller's robustness for the tracking in the disturbed environment, Mansour Karkoub et al.[21] proposed a hierarchical robust controller for the AUV target tracking. The controller applied back-stepping and sliding mode control technique for the hierarchical structure to realize controller's stability and robustness under disturbance. Taha Elmokadem et al.[22] made an analysis and comparison between the fast terminal sliding mode controller and the non-singular terminal sliding mode controller on their robustness.

Furthermore, neural network could help the controller improve its tracking performance through learning process. Zhouhua Peng et al.[23] designed an output feedback controller for the under-actuated AUV with an extended state observer, the projection neural network was proposed to optimize the controller's guidance signals. Zhenzhong Chu et al.[24] proposed a novel local recurrent neural network structure with fast learning speed for adaptive sliding mode controller in order to realize trajectory tracking for an ROV on the basis of unknown dynamic models.

However, during the target tracking process, the AUV or ROV should not only visually keep tracking with the target but also guarantee the target in the camera sight.[25] In the complicated submarine environment, it is more difficult to find the target once the vehicle following lost. In other words, autonomous target tracking requires the combination of perception and accurately tracking control. Currently, the development of artificial intelligence technology can help the autonomous system to percept, cognize, and react with the changing environment through machine learning techniques.[26] Marc et al.[27] proposed a novel semi-online neural-Q-learning controller to realize target tracking, through Q-learning algorithm the neural network computing control responses can be updated and improved. Moreover, controller with fuzzy rules and learning techniques are also conceived to be similar with human intelligence. Underwater vehicles can realize automatic target tracking and target in sight coordination through the learning based fuzzy systems.

Contributions of this work are as follows:

Firstly, in order to overcome the influence from occlusion and realize continuous long-term tracking, this paper proposed an improved KCF tracker with a self-discrimination mechanism based on

https://doi.org/10.1017/S0263574720001502 Published online by Cambridge University Press

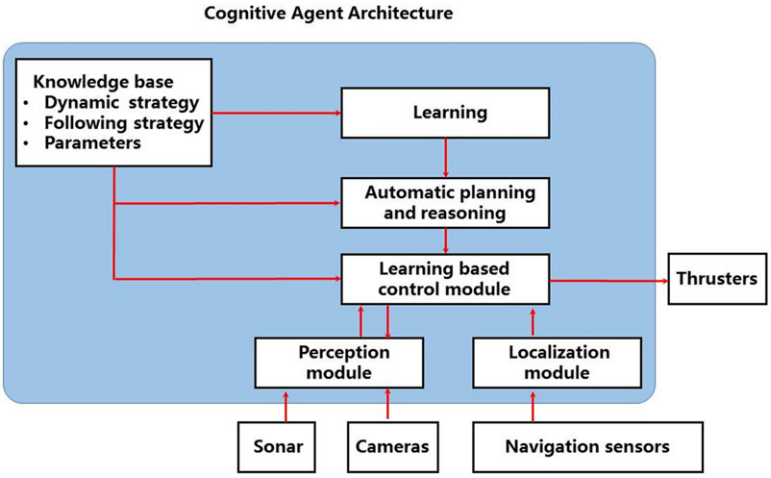


Fig. 1. Architecture for the remotely autonomous control of open frame underwater vehicle.

system confidence uncertainty. The mechanism can reinitialize the tracker through the detector when occlusion happens.

Secondly, a novel fuzzy logic tracking controller has been proposed to keep the target in sight during disturbance with the fuzzy rules automatically generated and optimized from the learning based PSO algorithm.

Thirdly, in order to prove visual tracking and following control algorithm, three cases experiments including channel following, pipe following, target tracking, and grasp manipulation have been made. Control parameters and control algorithms have been compared and discussed.

The rest of this paper is organized as follows: Section 2 will establish the remotely autonomous control architecture of open frame underwater vehicle. Section 3 will propose an improved KCF tracking algorithm. Section 4 will issue a novel fuzzy logic tracking controller with rule automatic generation method. Experiments will be introduced in Section 5 to present the results of target tracking and control. Conclusions will be given in Section 6.

2. Remotely Autonomous Control and Target tracking Architecture for the Open-frame Underwater Vehicle

In order to realize target detection, tracking, and manipulation tasks, the remotely autonomous architecture has been designed on the basis of open frame vehicle embedded system (see Fig. 1). The architecture is composed of 4 function modules: Learning module, Knowledge base module, automatic planning and reasoning module, learning based control module, localization module and target perception module which includes target detection and visual tracking algorithm. Each module subsystem operates with independent task progress and unified communication protocol.

The perception module will realize target perception and visual tracking through improved KCF tracking algorithm. This module can realize visual tracking throughout the images and help the controller module keep the target in sight. The localization module will provide the vehicle position information through dead reckoning from three-dimensional velocities and angular information from Doppler Velocity Log (DVL) and magnetic compass. This module can help the vehicle complete target tracking control process. Through the learning based control module, the vehicle can generate and optimize fuzzy rules according to current disturbance, keep the target stay in the sight, control the vehicle velocity and position. Therefore the architecture can realize target tracking control through artificial intelligence based on fuzzy control method.

3. Improved KCF Visual Tracking Algorithm

3.1. KCF module

In compare with traditional visual tracking algorithm, KCF visual tracking algorithm can extract richer sets of training samples through the application of dense sampling method. Instead of sparse

https://doi.org/10.1017/S0263574720001502 Published online by Cambridge University Press

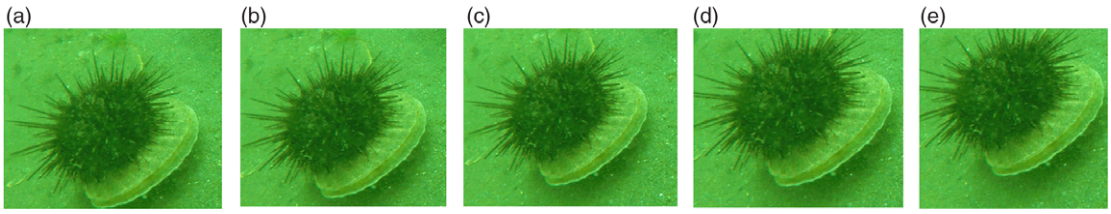


Fig. 2. Two-dimensional samples construction. (a) +30 pixels shift. (b) +15 pixels shift (c) Original image block of interest (d) −15 pixels shift (e) −30 pixels shift.

random sampling,[28] dense sampling is achieved by the cyclic shift of the base sample, which generates a sample loop matrix during the sampling process. According to the kernel function theorem,[29] a sample circulate matrix will be generated during the sampling process, and the sample circulate matrix still maintains the circulate characteristics after being mapped into the kernel space. The KCF visual tracking algorithm can greatly reduce the computational complexity and improve real-time tracking performance through the Fast Fourier Transform (FFT) according to the convolution theory.

In KCF tracker, the model is trained to learn an online CF from a plenty of positive and negative training samples, which are in a patch larger than twice size of the target ($M \times N$). The training samples are generated by all the cyclic shifts $S_{m,n}$, $(m, n) \in \{0, ..., M-1\} \times \{0, ..., N-1\}$ for the template estimation. However, this method cannot strictly distinguish the training samples between the positive and negative, and the desired output $y_{m,n}$ is constructed as a Gaussian distribution with its peak located at the tracked object centre and smoothly decayed to 0. The labels of the shifts are approximately equal to 1, which are closest to the base sample, while their opposites are close to 0.

Figure 2 illustrates a two-dimensional case that positive and negative sample sets are generated from the base sample. The original image block of interest is located at the middle of Fig. 2, while the images located at the left or right side of the image block are obtained by moving the original sample 15 and 30 pixels along the y axis positively or negatively. This process does not strictly distinguish positive from negative samples, but their samples subject to the Gaussian distribution. When the generated samples are close to the positive ones, their labels are closer to 1, otherwise, their labels are closer to 0.

The optimal solution w is the CF template, which is obtained through minimizing the regularized ridge regression error over the training samples $S_{m,n}$ and their labels $y_{m,n}$.

$$\min_{w} \sum_{i} \left| \left\langle \varphi(x_{m,n}), w \right\rangle - y_{m,n} \right|^2 + \lambda \left\| w \right\|^2 \tag{1}$$

where $y_{m,n}$ is compliant to Gaussian distribution, $\varphi(x)$ is the mapping from low-dimensional input space to the Hilbert space, the kernel function $\kappa(x, x') = \left\langle \varphi(x), \varphi(x)' \right\rangle$ represents a cross correlation of $\varphi(x)'$ and $\varphi(x)$ in high-dimensional space. $\lambda \geq 0$ is a regularization parameter to prevent over fitting.

After the non-linear mapping, the solution w can be represented as $w = \sum_{m,n} \alpha_{m,n} \varphi \left(x_{m,n} \right)$, then the dual solution is α:

$$\hat{\alpha} = \frac{\hat{y}}{\hat{k}^{xx} + \lambda} \tag{2}$$

where we denote the vector in the Fourier domain with a hat. $k^{xx'} = \kappa(x, x')$ is the CF of the appearance model. For an image patch with C feature channels and base sample as $\boldsymbol{x} = [x_1, x_2, x_3, ..., x_C]$, Gaussian kernel is selected to calculate the correlation:

$$k^{xx'} = \exp\left(-\frac{1}{\sigma^2} \left(||\boldsymbol{x}||^2 + ||\boldsymbol{x}'||^2 - 2F^{-1} \left(\sum_{c=1}^{C} \hat{x}_c \bullet (\hat{x}'_c)^* \right) \right) \right) \tag{3}$$

Where $\bullet$ is the element-wise product and F^{-1} is the inverse of discrete Fourier transform.

https://doi.org/10.1017/S0263574720001502 Published online by Cambridge University Press

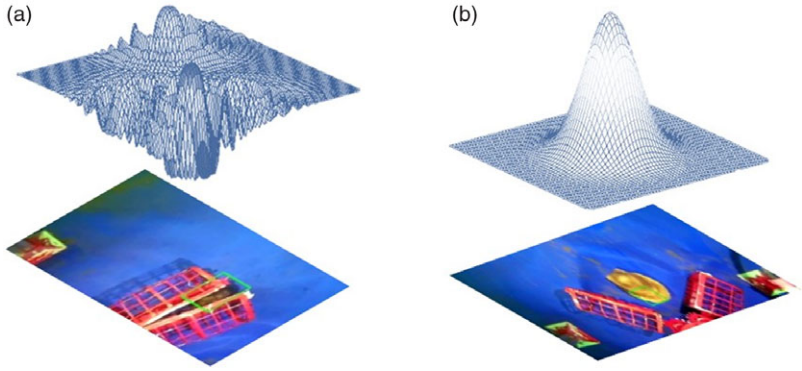


Fig. 3. The visualization of different response maps from the occlusion is updated per frame and follows the first order Markov process, the inference of the current target state is only related to the previous target frame state. The occlusion will lead to tracking mistake from the target to the robotic hand. (a) Occluded. (b) Normal.

In the next frame, a base sample z with the same size as x is cropped out. All the cyclic patches of z will calculate the cross correlation with the present model appearance x^* via

$$y = F^{-1}(k^{x^*z} \bullet \hat{\alpha}) \tag{4}$$

The patch with maximum score is the target position in the current frame.

3.2. Improved KCF tracking with feedback module

KCF tracker is a typical tracker of CF trackers with highspeed and favorable accuracy. However, it is not robust enough when handle with severe occlusions in the real-time underwater applications. For example, during the target grasping process, the target is sometime occluded by the movement of the robotic hand (see Fig. 3). As a result, the appearance model of the tracking object changes drastically due to severe occlusion. Since the appearance model of KCF.

As assumed earlier, the desired output $y_{m,n}$ and the ideal response map is compliant to Gaussian distribution, with only one single peak. The thinner peak value of the response, the lower confidence of the occlusion. Conversely, the entire response map will fluctuate drastically. On the other hand, the response map can reflect the degree of the occlusion. Thus this paper proposes an added self-discrimination (AS) mechanism based on system confidence uncertainty,

$$AS = \frac{|f_{\max} - f_{ave}|}{mean \sum_{x,y} |f_{xy} - f_{ave}| + \delta} \tag{5}$$

where f_{xy} denote the x-th row and y-th column element , $f_{\max}$, and f_{ave} denotes the maximum value and the mean value of the current frame response respectively. δ is an extremely low hyper parameter. When the AS is lower than a predefined threshold continuously in 100 frames, we assume the occlusion happens and reinitialize the tracker through the detector.[30]

4. Robust Fuzzy Logic Target tracking Control

Although conventional Proportional Integration Differentiation (PID) controllers are widely used, linear fixed gain usually cannot provide satisfactory performance. On the other hand, fuzzy logic control system can cope with non-linear system with dynamic uncertainties. The conventional fuzzy control method is illustrated in Fig. 4, where e is the target tracking error vector. The vector includes the horizontal errors in the rectangular coordinate or in polar coordinate. $\dot{e}$ is their changing rate vector of e. K_e and K_d are the input scale and differential factors, K_{pi} and K_{pd} are the output scaling factors. The controller tries to involve expert knowledge to construct a set of linguistic rules.

4.1. Fuzzification

The fuzzification process of this controller involves a scale mapping between the input variables and corresponding discourse. The input of the controller includes the error vector and error change vector

https://doi.org/10.1017/S0263574720001502 Published online by Cambridge University Press

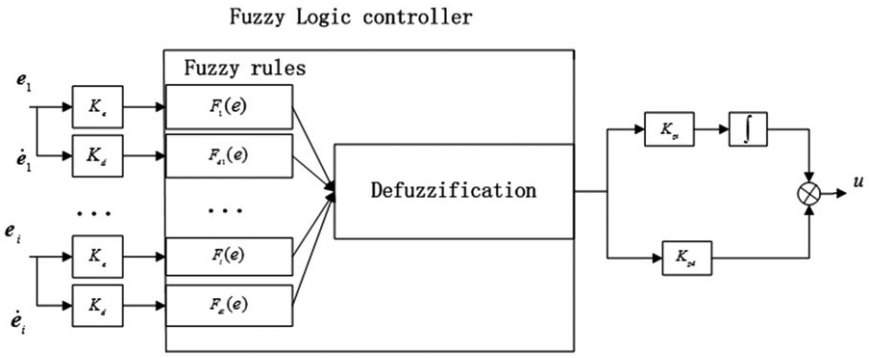


Fig. 4. Structure of fuzzy logic PID controller.

of target tracking. Conventional fuzzy linguistic labels include Positive Large (PL), Positive Medium (PM), Positive Small (PS), Zero (Z), Negative Small (NS), Negative Medium (NM), and Negative Large (NL). The triangular type membership function is selected for fuzzy sets:

$$\mu_{NPM}(x) = \begin{cases} 0 & x \le a_i \\ \dfrac{x - a_i}{b_i - a_i} & \\ \dfrac{c_i - x}{c_i - b_i} & b_i \le x \le c_i \\ 0 & c_i \le x \end{cases}$$

$$\mu_{NL}(x) = \begin{cases} 1 & x \le b_i \\ \dfrac{c_i - x}{c_i - b_i} & b_i \le x \le c_i \\ 0 & c_i \le x \end{cases}$$

$$\mu_{PL}(x) = \begin{cases} 0 & x \le a_i \\ \dfrac{c_i - x}{c_i - b_i} & a_i \le x \le b_i \\ 1 & b_i \le x \end{cases} \tag{6}$$

where $NPM \in \{NM, NS, Z, PS, PM\}$, x is the fuzzified crisp variable, a_i, b_i, and c_i are the ith triangular breakpoints.

4.2. Fuzzy rules initialization and optimization

For non-linear underwater target tracking in complicated environment, appropriate fuzzy rules correspondent to the real-time environment and vehicle state are very important to realize robust control. The initial fuzzy rules are derived from the rule base of Table I.

In order to optimize the fuzzy rules for complicated tracking state and environmental disturbance, the fuzzy rules are coded into particles including input variables (see Fig. 5). The best parameters of fuzzy system can be determined for the cooperative best value. The fitness value is assigned in the following:

I. Initialization: Fuzzy rules have been divided and coded into particle swarms. The particles are randomly selected corresponding to fuzzy rules from particle swarms.
II. Fitness value evaluation: In this study, the target tracking operation demands the controller to generate large output when the following deviation is relatively great, and strictly small output when the following deviation is relatively small. Thus the fitness function can be obtained according to S surface function:

$$u = \frac{2}{1 + \exp(-k_p e - k_d \dot{e})} - 1 \tag{7}$$

https://doi.org/10.1017/S0263574720001502 Published online by Cambridge University Press

Table I. Size and maneuverability parameters for the three AUVs.

	PL	**PM**	**PS**	**Z**	**NS**	**NM**	**NL**
NL	Z	NS	NM	NL	NL	NL	NL
NM	PS	Z	NS	NM	NL	NL	NL
NS	PM	PS	Z	NS	NM	NL	NL
Z	PL	PM	PS	Z	NS	NM	NL
PS	PL	PL	PM	PS	Z	NS	NM
PM	PL	PL	PL	PM	PS	Z	NS
PL	PL	PL	PL	PL	PM	PS	Z

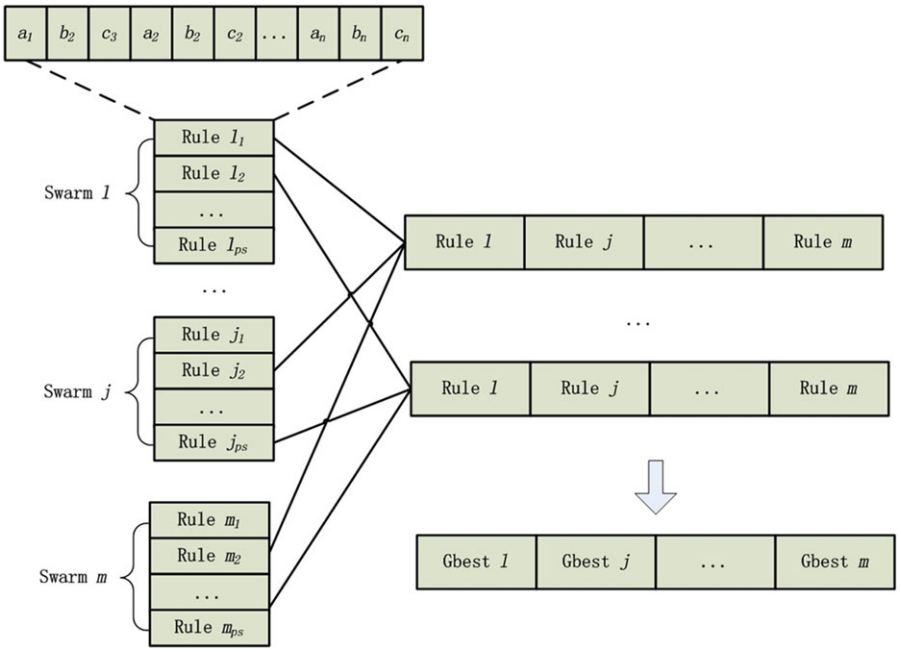


Fig. 5. Structure of particle rule optimization.

where k_p and k_d are the proportional and derivative gains. Therefore, the following fitness function is defined as:

$$FIT = \sum_{i=1}^{m} \left| \frac{k_e(|e_i| + |\dot{e}_i|)}{k_u(\frac{2}{1+\exp(-k_p e_i - k_d \dot{e}_i)} - 1) - y_{outi}} \right| \tag{8}$$

where k_e and k_u are the adjustable variables, e_i and y_{outi} are the error and corresponding output of fuzzy rule.

III. Particle optimization and selection: In this stage, each rule particle is evaluated through its fitness value. In the Particle Swarm Optimization (PSO) algorithm, each particle adjusts its status and searches for the optimal solutions according to the particle experiences. The improved PSO algorithm is defined as:

$$\begin{cases} v_k^c(t+1) = \omega v_k^c(t) + c_1 \times r_1 \times \left(P_{best_k^d} - p_k^c(t)\right) + \\ \qquad\qquad c_2 \times r_1 \times \left(p_k^c(t) - P_{worst_k^d}\right) + \lambda_3 \times r_1 \times \left(G_{best_k^d} - p_k^c(t)\right) \\ x_k^c(t+1) = p_k^c(t) + v_k^c(t+1) \end{cases} \tag{9}$$

Where $P_{best_k^d}$ and $G_{best_k^d}$ represent the best previous position of the kth rule particle and the best previous position of all the rule particles in the swarm respectively, $P_{worst_k^d}$ represents the

https://doi.org/10.1017/S0263574720001502 Published online by Cambridge University Press

worst previous position for the kth rule particle, $p_k^c(t)$ represents the kth rule particle position at current status, r_1 represents the random number of [0, 1], ω, c_1 and c_2 are inertial coefficients. Through these three stages above, each particle is continuously modified and optimized until the best fitness fuzzy rule value is obtained.

IV. Particle individual learning: Since the standard PSO suffers from premature convergence and high computation cost problems, reinforcement learning for particle individuals will be performed in this step to improve the particle operations. The following Q-learning algorithm is purposed to predict and optimized rule particles through mapping the state and selecting the action pairs. The action pairs including the action rules correspondent to current vehicle state.

In the Q-learning algorithm, the fuzzy rules are acquired through estimating the value of $Q_t(s(t), a(t))$ for each state and action pairs. The process of Q-learning is illustrated in the following:

Step ① Initialize the vehicle current state $s(t)$.
Step ② The vehicle takes an action $a(t)$ according to ε-greedy method.
Step ③ The vehicle receives next state $s(t+1)$ and a reward $r(t+1)$ from the environment.
Step ④ The vehicle updates its Q-value $Q_t(s(t), a(t))$ for state $s(t)$ and action $a(t)$ by:

$$\begin{aligned} &Q_{t+1}(s(t), a(t)) \\ &\quad = Q_t(s(t), a(t)) + \alpha \left[r(t+1) + \gamma Q_{best}(s(t+1)) - Q_t(s(t), a(t)) \right] \end{aligned} \tag{10}$$

where α is the learning rate, γ is the discount parameter, $\gamma \in [0, 1]$, $r(t+1)$ is the immediate reinforcement reward, $Q_{best}(s(t+1))$ is the best estimation of $Q_t(s(t+1))$ value. The Q value will be updated as:

$$\Delta Q = r(t+1) + \gamma Q^*(s(t+1)) - Q(s(t), a(t)). \tag{11}$$

Based on Eq. (11), each particle is further modified. and steps ①, ②, ③ and ④ are repeated iteratively until G_{best} is obviously improved. The particle with best fitness of P_{best} is the global best one G_{best^d}. Therefore the best fuzzy rule will be obtained to deal with environmental disturbance and vehicle state change during capturing process.

4.3. Defuzzification

In the defuzzification process, the output of the defuzzification equation is defined as the weighted average of the fuzzy outputs:

$$\boldsymbol{u} = \frac{\int \mu_p(\boldsymbol{u}_{pi}) \boldsymbol{u}_{pi} du}{\int \mu_p(\boldsymbol{u}_{pi}) du} \tag{12}$$

where μ_p is the weight value, $\boldsymbol{u}_{pi}$ is the center value of the output fuzzy set for the ith rule particle.

5. Experimental Results of Visual Tracking and Target Tracking Control

5.1. Experimental setup

In order to verify the performance of visual tracking algorithm and target tracking control, an open frame underwater vehicle of Fig. 6 has been applied for the experiments. This vehicle is 900 mm long, 750 mm wide and 600 mm high. The vehicle weighs 80 kg, with the depth rating at 100 m. It is equipped with 4 vector thrusters for horizontal movement and two vertical thrusters for diving. The motion sensor for navigation includes a magnetic compass and a DVL, while the environmental sensor including three 1280*720p cameras and three distant measurement sonars for environmental detection and visual tracking. Moreover the vehicle is equipped with a 2-joint manipulator for underwater manipulation. In order to realize remotely autonomous detection and control operation, the open frame underwater vehicle is equipped with a tether responsible with the optical communication and power supply. The control system structure of the vehicle including underwater low-level control unit and surface autonomous detection & control unit. The core of underwater low level

https://doi.org/10.1017/S0263574720001502 Published online by Cambridge University Press

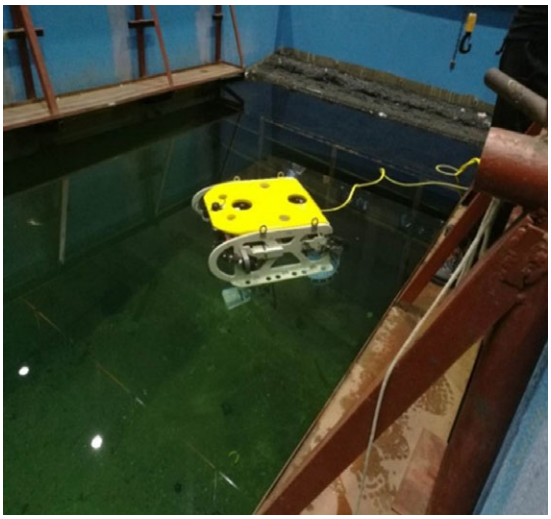


Fig. 6. Open frame underwater vehicle platform.

control unit is PC104 embedded processor which is responsible for the sensor information sampling and vehicle position control. The surface autonomous detection and control unit can process the message from environmental sensors and realize autonomous target detection, visual tracking and autonomous manipulation control. For the parameter selections, the proportional and derivative gains $k_e, k_d \in [0, 100]$, the selection of proportional and derivative gains can coordinate the fitness function for the particles, $k_u, k_e \in [0, 1]$; for the PSO $\lambda_3 = 0.6$, $c = c_2 = 2.06$ the population size are selected as 200 for the improvement and speed, the iteration times are 310 times for PSO and online Q-learning, the learning parameter $\gamma = 0.78$, $\alpha = 0.4$.For the self-discrimination criterion of AS, the discrimination occlusion of time is selected as 100, which is a compromise between tracking accuracy and grasping efficiency. The longer the time, the lower the grasping efficiency. In order to make more comprehensive discussions, comparisons have been made between ref. [28] with Camshift algorithm on visual tracking and a fuzzy logic controller for target following.

5.2. Case study for target tracking control

5.2.1. Wall following experiments in the channel. For the inland channel, the wall following is very important to detect the wall of channel. The open frame underwater vehicle is equipped with three distant measurement sonars to ascertain he distance between underwater vehicle and the wall. In the channel wall following experiments of Fig. 7(b), the start point is (1, −10), the end point is (−10, −5). The expected distance between the underwater vehicle and channel wall is 2 m (see Fig. 7(c)). In compare with traditional fuzzy control results, the adaptive PSO optimized fuzzy controller can obtain the most reasonable trajectory for the wall following. From Fig. 7, the traditional fuzzy controller cannot adapt to the environmental disturbance (see Fig. 7(a)) and the dynamically changed channel wall, the fixed rules usually lead to late and inflexible responses, thus the more complicated conditions for the disturbance and the turning of the wall the greater will be the errors. The PSO algorithm with fuzzy rules optimization embodies its advantage in the rule changing according to the real state; moreover, the designed fitness function can redesign fuzzy rules to control the vehicle reaching the desired position quickly and maintain stable states in the disturbance environment. From another channel following experiments of Fig. 8, further discussions on control parameters' effects have been made. The reduce of λ_3 and learning rate α can enlarge the control errors, while the increase of λ_3 and learning rate α can reduce the control errors, but may introduce control vibrations because learning more frequently and the particles vary more quickly.

5.2.2. Pipelines following experiments in the tank. The pipelines following experiments have been performed in a 50 × 30 × 10 m tank with wave and local current generation device (see Fig. 9) in Harbin Engineering University. The pipeline inspection following experiment was made in current disturbance with the speed at 0.5 m/s. The following process is realized through the pipeline contour detection and extraction. During the following process, the offset distance and angle of

https://doi.org/10.1017/S0263574720001502 Published online by Cambridge University Press

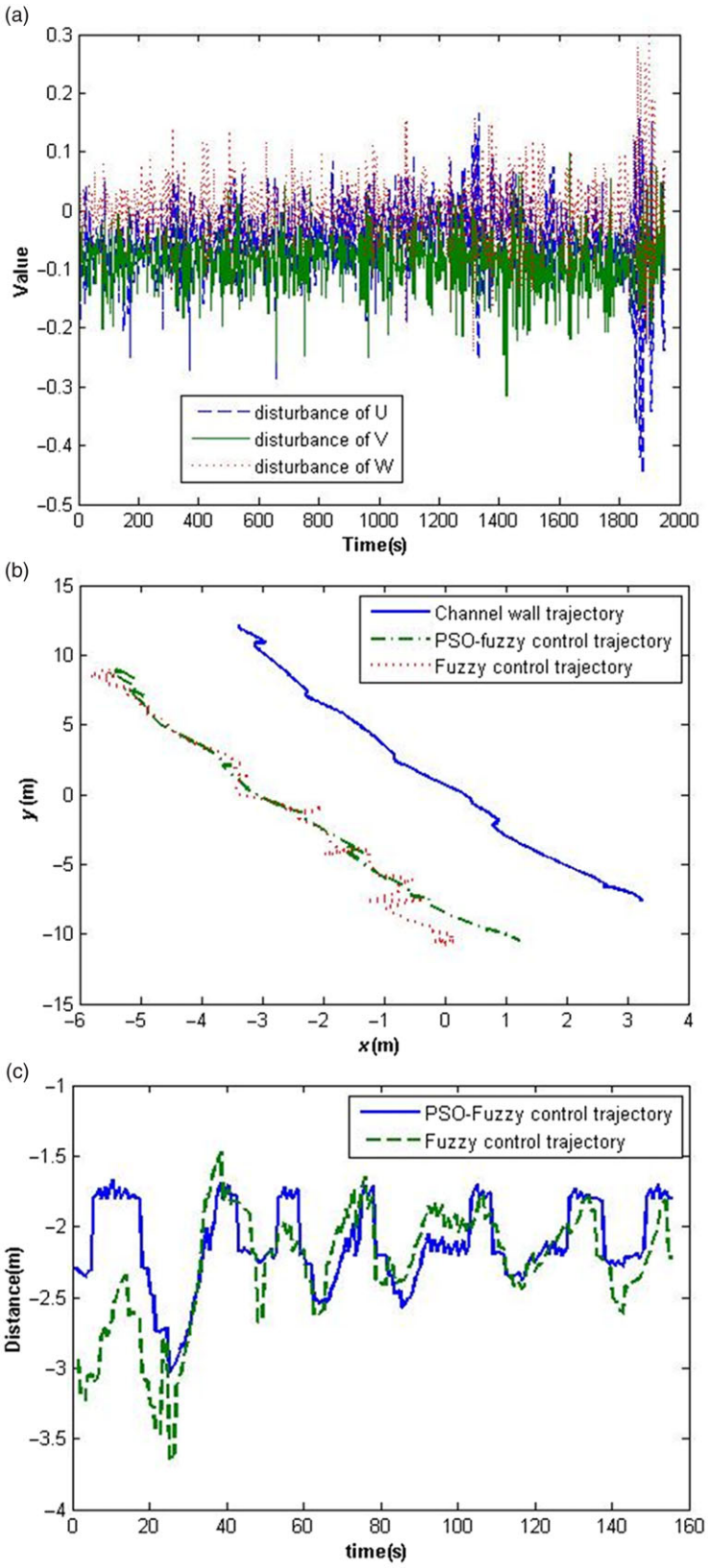


Fig. 7. Wall following experiments in the channel. (a) Environmental disturbance obtained from DVL. (b) Channel following results. (c) Real-time distance between the underwater vehicle and the channel.

https://doi.org/10.1017/S0263574720001502 Published online by Cambridge University Press

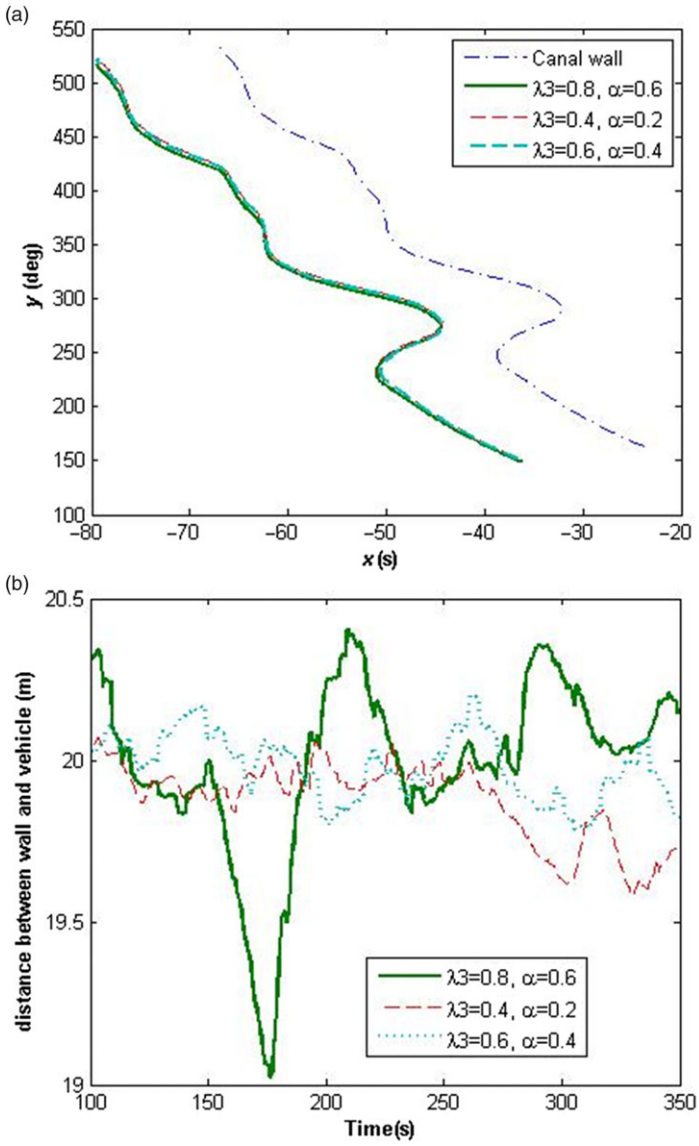


Fig. 8. Wall following comparison experiments in the channel. (a) Channel following results. (b) Real-time distance between the underwater vehicle and the channel.

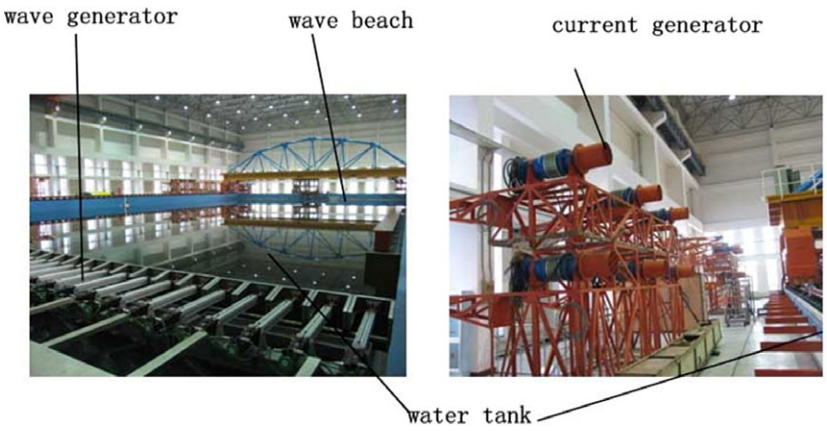


Fig. 9. Wave generator and local current generation device.

https://doi.org/10.1017/S0263574720001502 Published online by Cambridge University Press

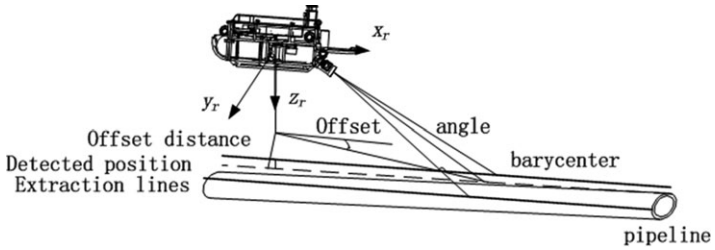


Fig. 10. Pipeline inspection principle.

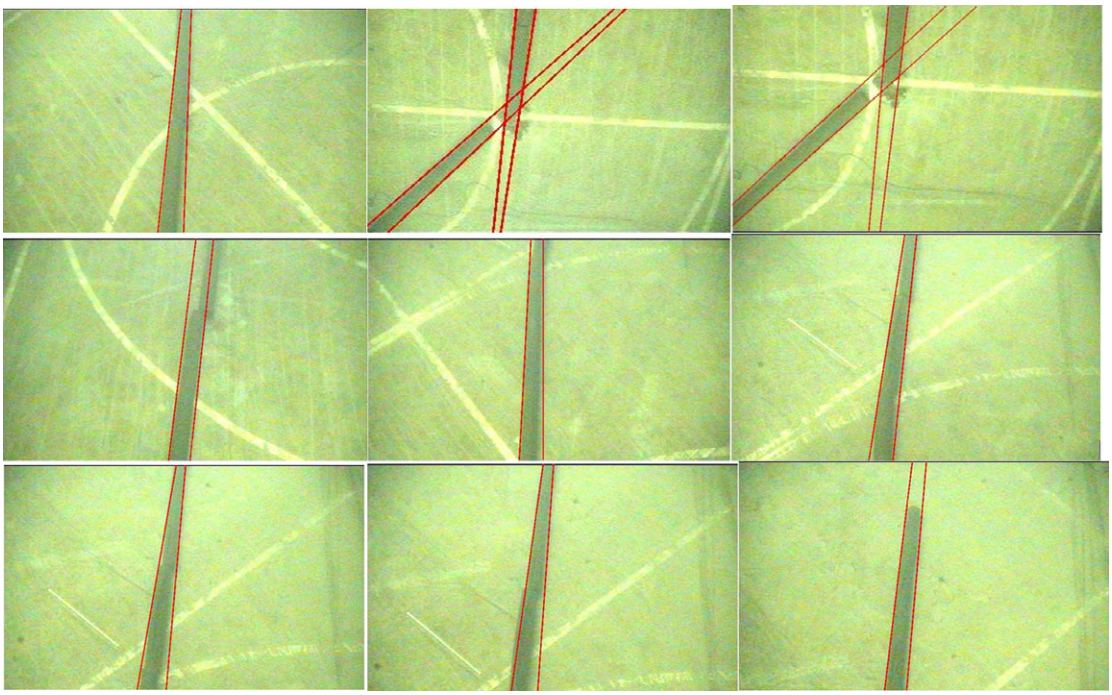


Fig. 11. Pipeline contour extraction.

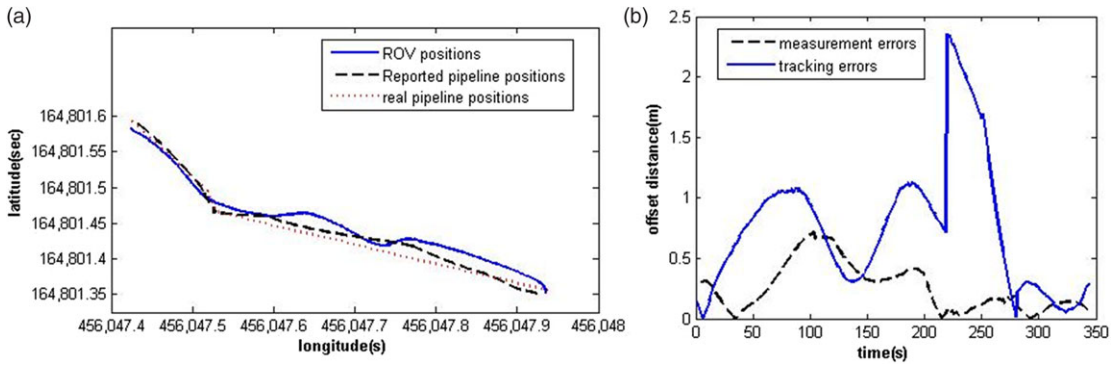


Fig. 12. Pipeline inspection results (a) Horizontal slices measurement path (b) Measurement Results.

pipeline tracking were obtained through the comparison between the midline of pipe contour and the trace of underwater vehicle (see Figs. 10 and 11). Figure 12(a) illustrates the pipeline tracking path and tracker reported pipeline positions by underwater vehicle in the disturbance environment. Figure 12(b) illustrates the tracking errors and position measurement errors relative to the actual pipeline positions. The following results illustrated precise following control results in the disturbance environment.

https://doi.org/10.1017/S0263574720001502 Published online by Cambridge University Press

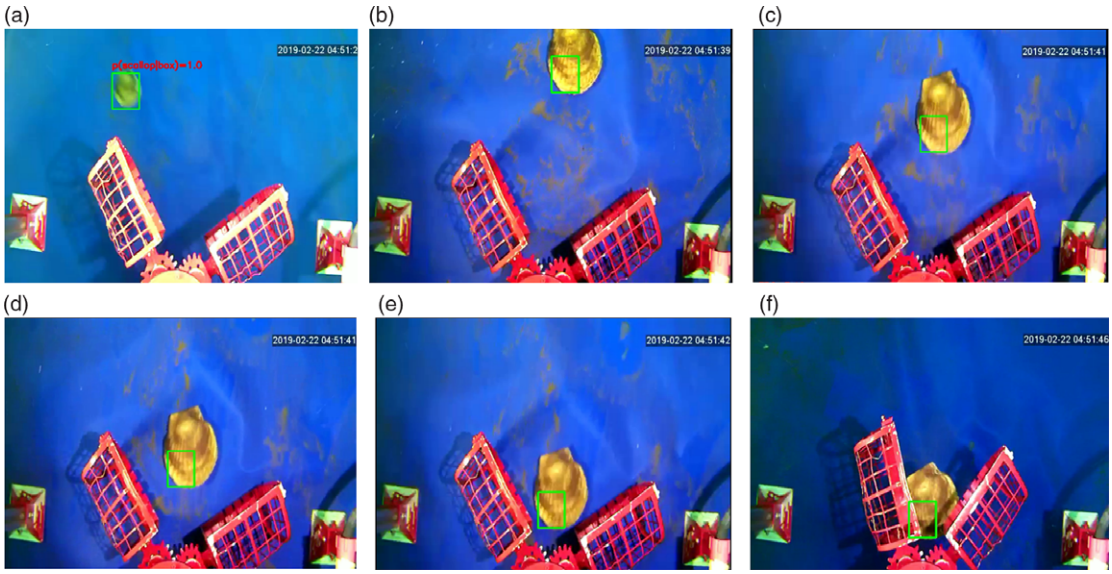


Fig. 13. The autonomous grasping process.

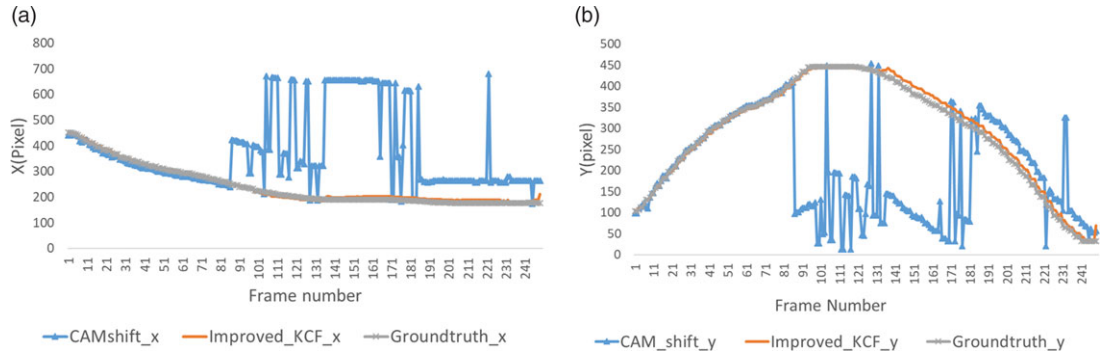


Fig. 14. Short term tracking results.

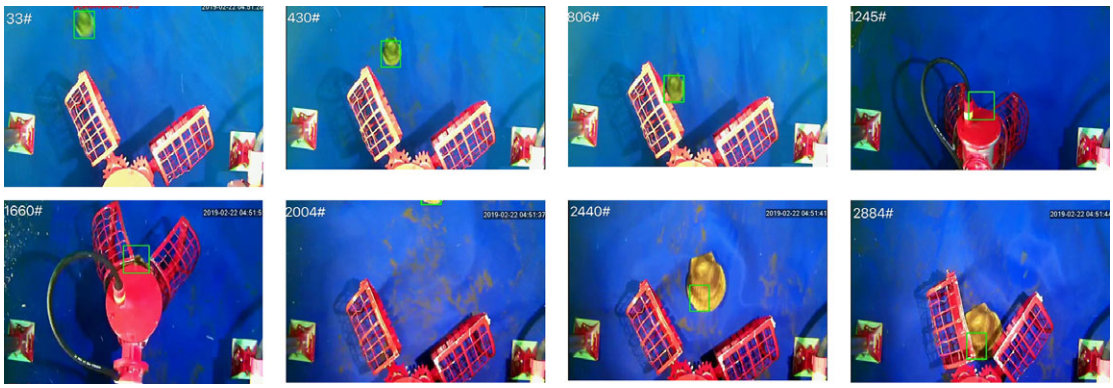


Fig. 15. Long time continuous tracking results.

5.3. Case study for underwater manipulation

The experiments for target tracking are performed in the tank of 50 × 30 × 10 m (length × width × depth). Visual tracking is performed on the basis of a RTX2070 notebook with 3.2 GHz Intel Core i7. We adopt the HOG feature as the feature representation, which is represented by a nine-bin histogram in each cell. The threshold of AS is set as 0.1 in the tank experiments. Other basic parameter settings such as the Gaussian kernel are consistent with the ref. [31].

https://doi.org/10.1017/S0263574720001502 Published online by Cambridge University Press

The following is an experiment about the sea organism target tracking and grasp control on the basis of the open frame underwater vehicle of Fig. 6. The tracking performance is evaluated by the two-dimension spatial distance between the center of the tracking target and the ground truth. As shown in Figs. 13 and 14, the vehicle has successfully recognized (see the first figure of Fig. 13) and tracked the target through improved KCF tracker in order to capture the target (see the last figure of Fig. 13) through the proposed controller. In Fig. 14, the gray lines represent the ground truth of target motions in the x and y axes, the blue lines represent the tracking results of the Camshift[28] tracker, the red lines represent the tracking results of the improved KCF tracker. It can be observed that our improved KCF tracker has significantly outperforms the Camshift tracker in the target tracking tasks. Instead of sparse random sampling,[28] a large number of sample loop matrix are generated during the sampling process, which is a key factor of the robustness.

To illustrate the long-term tracking results, we apply the proposed KCF tracker and controller in Fig. 15. The target tracking and grasp process last for 128 s with 3200 frames tracking pictures. In the process, the shell fish target has firstly been recognized and tracked. At the 1200 frame, the target has been occluded by hand. When the occlusion lasts for more than 100 frames, the tracker will assume the occlusion happens and reinitialize the tracker through the detector. Therefore, the proposed tracker and controller can successfully make continuously tracking and target grasp.

6. Conclusions

Visual tracking is very important for target detection and grasp. This paper has proposed an open frame underwater vehicle with remotely autonomous tracking architecture. In order to overcome the influence from occlusion, an improved KCF tracker has been proposed with an added self-discrimination mechanism based on system confidence uncertainty, which realized long term and continuous tracking. Furthermore, an S surface based function has been designed in the improved PSO algorithm. The improved PSO algorithm can generate optimized fuzzy rules for stable tracking control so that stable tracking can be realized in the face of different environmental disturbances. Tank and channel experiments of target tracking and grasp have been carried out to verify the designed tracker and controller on the basis of remotely autonomous underwater vehicle. The future work will focus on the deep learning based underwater target tracking and grasp control with obstacles.

Acknowledgements

This project is supported by National Nature Science Foundation of China (No. 61633009, 51579053, 51209050, 51639004, 61603277, 51779052, 51779059), the Community Technology (No.41412050101) and Field Fund (No.61403120301) of the 13th Five-Year Plan for Equipment Pre-research Fund, and also funded by the Key Basic Research Project of "ShanghaiScience and Technology Innovation Plan" (No.15JC1403300).

References

1. J.-g. Shi, D.-j. Li and C.-j. Yang, "Design and analysis of an underwater inductive coupling power transfer system for autonomous underwater vehicle docking applications," *J. Zhejiang Univ. Sci. C (Comput. Electron.)* **15**(1), 51–62 (2014).
2. Y. Li, R. Cui, Z. Li and D. Xu, "Neural network approximation based near-optimal motion planning with kinodynamic constraints using RRT," *IEEE Trans. Ind. Electron.* **65**(11), 8718–8729 (2018).
3. E. Peymani and T. I. Fossen, "Path following of underwater robots using lagrange multipliers," *Rob. Auton. Syst.* **67**, 44–52 (2015).
4. H. Qin, H. Chen and Y. Sun, "Distributed finite-time fault-tolerant containment control for multiple Ocean Bottom Flying Nodes," *J. Franklin Inst.* (2019). https://doi.org/10.1016/j.jfranklin.2019.05.034.
5. G. Ferri, A. Munafò and K. D. LePage, "An autonomous underwater vehicle data-driven control strategy for target tracking," *IEEE J. Oceanic Eng.* **43**(2), 323–343 (2018).
6. S. A. Villar1, G. G. Acosta, A. L. Sousa and A. Rozenfeld, "Evaluation of an efficient approach for target tracking from acoustic imagery for the perception system of an autonomous underwater vehicle," *Int. J. Adv. Rob. Syst.* **11**(1), 1–13 (2014).
7. L. Lapierre and B. Jouvencel, "Robust non-linear path-following control of an AUV," *IEEE J. Oceanic Eng.* **33**(2), 89–92 (2008).
8. J. Gao, "Transfer Learning Based Visual Tracking with Gaussian Processes Regression," *Proceedings of European Conference on Computer Vision* (2014) pp. 188–203.
9. S. Hare, "Struck: Structured Output Tracking with Kernels," *Proceedings of International Conference on Computer Vision* (2011) pp. 263–270.

https://doi.org/10.1017/S0263574720001502 Published online by Cambridge University Press

10. B. Babenko, "Robust object tracking with online multiple instance learning," *IEEE Trans. Pattern Anal. Mach. Intell.* **33**(8), 1619–1632 (2011)
11. S. Hong, "Online Tracking by Learning Discriminative Saliency Map with Convolutional Neural Network," *Proceedings of International Conference on Machine Learning* (2015) pp. 597–606.
12. L. Wang, "Stct: Sequentially Training Convolutional Networks for Visual Tracking," *Proceedings of Conference on Computer Vision and Pattern Recognition* (2016) pp. 1373–1381.
13. L. Wang, "Visual Tracking with Fully Convolutional Networks," *Proceedings of International Conference on Computer Vision* (2015) pp. 3119–3127.
14. F. H. Sun, "Stability control for the head of a biomimetic robotic fish with embedded vision," *Robot*. **37**(2), 188–203 (2015).
15. D. Bolme, "Visual Object Tracking Using Adaptive Correlation Filters," *Proceedings of IEEE Conference on Computer Vision and Pattern Recognition* (2010) pp. 2544–2550.
16. J. Henriques, "Exploiting the Circulant Structure of Tracking-by-Detection with Kernels," *Proceedings of 12th European Conference on Computer Vision* (2012) pp. 702–715.
17. R. J. Huang, "Applying Convolutional Networks to Underwater Tracking without Training," *Proceedings of IEEE International Conference on Applied System Innovation 2018* (2018) pp. 342–345.
18. B. Subudhi, K. Mukherjee and S. Ghosh, "A static output feedback control design for path following of autonomous underwater vehicle in vertical plane," *Ocean Eng.* **63**, 72–76 (2013).
19. X. Qi, "Spatial target path following control based on Nussbaum gain method for underactuated underwater vehicle," *Ocean Eng.* **104**, 680–685 (2015).
20. C. Shen, B. Buckham and Y. Shi, "Modified C/GMRES algorithm for fast nonlinear modeln predictive tracking control of AUVs," *IEEE Trans.Control Syst. Technol.* **25**(5), 1896–1904 (2017).
21. M. Karkoub, H.-M. Wu and C.-L. Hwang, "Nonlinear trajectory-tracking control of an autonomous underwater vehicle," *Ocean Eng.* **145**, 188–198 (2017).
22. T. Elmokadema, M. Zribia and K. Youcef-Toumi, "Terminal sliding mode control for the trajectory tracking of underactuated autonomous underwater vehicles," *Ocean Eng*. **129**, 613–625 (2017).
23. Z. Chu, D. Zhu and S. X. Yang, "Observer-based adaptive neural network trajectory tracking control for remotely operated vehicle," *IEEE Trans. Neural Networks Learn. Syst.* **28**(7), 1633–1645 (2017).
24. Z. Peng and J. Wang, "Output-feedback path-following control of autonomous underwater vehicles based on an extended state observer and projection neural networks," *IEEE Trans. Syst. Man Cybern. Syst.* (Accepted).
25. E. H. C. Harik, F. Guérinc, F. Guinand, J.-F. Brethé, H. Pelvillan and J.-Y. Parédé, "Fuzzy logic controller for predictive vision-based target tracking with an unmanned aerial vehicle," *Adv. Rob.* **31**(7), 368–381 (2017).
26. E. Galceran, R. Campos, N. Palomeras, D. Ribas, M. Carreras and P. Ridao, "Coverage path planning with real-time replanning and surface reconstruction for inspection of three-dimensional underwater structures using autonomous underwater vehicles," *J. Field Rob.* **32**(7), 952–983 (2015).
27. M. Carreras, J. Yuh, J. Batlle and P. Ridao, "A behavior-based scheme using reinforcement learning for autonomous underwater vehicles," *IEEE J. Oceanic Eng.* **30**(2), 416–427 (2005).
28. Y. Hu, W. Zhao, G. Xie and L. Wang, "Development and target following of vision-based autonomous robotic fish," *Robotica* **27**, 1075–1089 (2009).
29. P. Davis, *Circulant Matrices* (American Mathematical Society, New York, 1979).
30. H. Hai, Z. Hao, Y. Xu, Z. Lu, L. Qi and A.-Y. Zang, "Faster R-CNN for marine organisms detection and recognition using data augmentation," *Neurocomputing* **337**, 372–384 (2019).
31. J. F. Henriques, "High-speed tracking with kernelized correlation filters," *IEEE Trans. Pattern Anal. Mach. Intell.* **37**(3), 583–596 (2015).

https://doi.org/10.1017/S0263574720001502 Published online by Cambridge University Press